Liquid water ionization by fast electron impact: a multiple differential study for the $1B_1$ orbital

2012 J. Phys. B: At. Mol. Opt. Phys. 45 045206

(http://iopscience.iop.org/0953-4075/45/4/045206)

J. Phys. B: At. Mol. Opt. Phys. **45** (2012) 045206 (8pp) doi:10.1088/0953-4075/45/4/045206

Liquid water ionization by fast electron impact: a multiple differential study for the $1B_1$ orbital

M L de Sanctis[1], M-F Politis[2], R Vuilleumier[3], C R Stia[1] and O A Fojón[1]

[1] Instituto de Física Rosario (CONICET-UNR), Av. Pellegrini 250, 2000 Rosario, Argentina
[2] Laboratoire Analyse et Modélisation pour la Biologie et l'Environnement, CNRS UMR 8587, Université d'Evry Val d'Essonne, Boulevard François Mitterrand 91025 Evry, France
[3] École Normale Supérieure, Département de Chimie, UMR 8640 CNRS-ENS-UPMC, 24, rue Lhomond, 75005 Paris, France

E-mail: ofojon@fceia.unr.edu.ar

Received 8 November 2011, in final form 23 December 2011
Published 7 February 2012
Online at stacks.iop.org/JPhysB/45/045206

Abstract
We study theoretically the single ionization of water molecules in a liquid phase by impact of fast electrons in a coplanar geometry. For the first time, the wavefunction for a single water molecule in the liquid phase is described in a realistic way by means of a Wannier orbital formalism. Multiple differential cross sections for the most external $1B_1$ orbital are obtained through a first-order model within the framework of an independent electron approximation. Moreover, the relaxation of the target is not taken into account. We compare our results with previous theoretical and experimental ones for water in a gas phase. The main physical features of the reaction observed in measurements for vapour (such as binary and recoil peaks) are also observed in our theoretical predictions.

(Some figures may appear in colour only in the online journal)

1. Introduction

The ionization of water molecules is a basic reaction of relevance in several domains such as radiobiology, radioprotection and medical physics [1, 2]. As water is the main component of the biological matter, the study of this reaction is crucial to understand the damage provoked to living tissue by the ionizing radiations. It is nowadays well established that there exist strong links between the exposition to them and the biophysical processes that induce complex DNA lesions as well as gene and chromosomal mutations. In particular, the production of low-energy secondary electrons resulting from a primary ionization of water is of importance to elucidate the mechanisms that lead to cell alteration [3]. Although ionization of water molecules in a gas phase by electron impact has been studied in several works [4–13], only recently have a few been devoted to the study of liquid water ([14–16], see also [17] and references therein). Moreover, in simulations of the passage of ionizing radiations through living matter, the liquid phase is very often replaced by the gas phase to simplify the corresponding track structure analysis. Accordingly, a realistic description of the ionization of water molecules in the proper thermodynamical phase of the biological environment is required.

Therefore, we study in this work the single ionization of water molecules in the liquid phase by electron impact at intermediate and high incident energies. The appropriate representation of molecules in the liquid phase is a difficult task that added to the particularities of the collision problem (involving, for instance, the correct treatment of the Coulomb asymptotic behaviour of the interactions between charged fragments in the final channel) turns it practically irresoluble. In consequence, several approximations are required to obtain the observables of the reaction (i.e. the multiple differential cross sections (MDCS)) in order to have a first approach to the dynamics of the (e,2e) process.

Taking into account the above-mentioned considerations, we present a simple monoelectronic first-order model. To represent the initial state of an isolated water molecule in the liquid phase, we employ for the first time wavefunctions

obtained by means of a Wannier orbital formalism that transforms the wavefunction of the whole liquid system into electronic orbitals localized over each water molecule in the liquid phase [18]. In this way, we obtain a realistic description of the liquid phase. To circumvent the complexities of the multielectron nature of the target, we use an independent electron approximation in which one electron (the *active* one) of the target is ejected in the final channel of the reaction whereas the other ones (the *passive* electrons) remain as frozen in their initial orbitals. We compute MDCS for the most external ($1B_1$) orbital of the water molecule. Previous results for the mentioned orbital, published in [16], are also included in this work. In addition, we compare our predictions with an enlarged set of experiments.

As experimental results of MDCS at fixed molecular orientations for liquid water are not available, we compare our theoretical predictions with other theoretical ones obtained for the gas phase [19]. These previous calculations correspond also to a first-order model in which the water orbitals in gas phase are obtained through a development centred on the heavy oxygen atom as given by Moccia [20]. In contrast, there exist measurements of MDCS for randomly oriented vapour water molecules [21]. So, we also present MDCS averaged over all the molecular orientations and compare them with those experiments to check if our model reproduces the main physical features of the experimental MDCS for the gas phase, i.e. the binary and recoil peaks. It is worthy to mention that the presence of the binary peak is verified in the case of *active* electrons coming from initial s orbitals, whereas for those coming from p ones, the binary peak may be split up into two lobes symmetric with respect to the direction of the momentum transfer. In addition, we also compare our predictions for the averaged MDCS with the ones from a recently developed model for liquid water [17]. This model is obtained also within the first Born approximation but differs with our model in the description of the initial orbitals for the liquid water which are described in [17] in a simpler manner through monocentric expansions in Gaussian basis.

Atomic units are used except where otherwise explicitly stated.

2. Theory

2.1. Effective molecular orbitals for liquid water

We describe here the effective molecular wavefunctions for a water molecule extracted from the liquid phase that we use in our cross-section calculations. The electronic state of the system is described in the framework of Kohn–Sham density functional theory and molecular orbitals are constructed from the occupied, extended, Kohn–Sham ones by using maximally localized Wannier functions [22, 23]. Details of the method can be found in [24, 18].

Briefly, we start with maximally localized Wannier orbitals w_i that are obtained by a unitary transformation $\mathbf{U}$ of the Kohn–Sham orbitals ψ_k,

$$w_i = \sum_k U_{ik}\psi_k, \tag{1}$$

such as the spatial spread of the resulting orbitals

$$\Omega = \sum_i [\langle w_i|\mathbf{r}^2|w_i\rangle - \langle w_i|\mathbf{r}|w_i\rangle^2] \tag{2}$$

is minimized [22]. In the preceding equations, $\mathbf{r}$ stands for the electron position operator and summations run over all the occupied Kohn–Sham states. While the orbitals ψ_k are delocalized over the whole system, losing thus the molecular picture, the Wannier functions w_i are local to specific molecules in the liquid. For a typical configuration, four doubly occupied Wannier orbitals can be assigned to each water molecule: two of them representing OH bonds and the other two describing lone pairs [25].

An intermediate representation has been introduced by Vuilleumier and co-workers [24] in which the orbitals are local to a molecule but delocalized within it. This intermediate representation is perhaps more appropriate for the study of condensed molecular systems [18]. In this scheme, effective molecular orbitals are obtained by grouping the Wannier orbitals assigned to a specific molecule and then diagonalizing the Wannier Hamiltonian in each molecular subspace [24, 18]. The resulting orbitals Φ_n can thus be expressed as

$$\Phi_n = \sum_i T_{ni}\, w_i, \tag{3}$$

where the summation is restricted to the valence electron functions of a single molecule. In the last equation, $\mathbf{T}$ represents the corresponding unitary transformation. The orbitals Φ_n are by construction localized on each water molecule and they result similar to the molecular orbitals of the isolated molecule in vacuum. Indeed, it was shown that the Kohn–Sham state of pure liquid water can be expressed through this method as a Slater determinant of four doubly occupied effective molecular orbitals (which through two successive unitary transformations are unitary transformed Kohn–Sham orbitals) per water molecule which can be unambiguously labelled $1A_1$, $1B_2$, $2A_1$ and $1B_1$ by similarity with the standard orbitals for a water molecule in vacuum [18].

In this work, calculations for the effective $1B_1$ orbital of a single water molecule in a liquid phase are performed. In the original work by Hunt *et al* [18], the liquid phase is simulated with a system consisting of 32 water molecules in a simple cubic periodic cell of dimension 18.6 au corresponding to the experimental density under ambient conditions. Such relatively small sample size is sufficient to correctly reproduce the structure of liquid water [26]. However, the obtained $1B_1$ wavefunction for this system turned out not to be sufficiently close to zero at the box boundaries. For the cross-section calculation, the spatial range of the initial bound wavefunction must be finite. For isolated targets, it is expected in general that the wavefunction asymptotically vanishes at about 10 au. In the liquid, the spherically averaged molecular density extracted from the Wannier orbitals decreases exponentially as expected for an insulator [27]; however, there are local fluctuations due to the orthogonality condition with orbitals from other molecules. In order to make the wavefunction sufficiently small everywhere on the boundaries in order to perform realistic calculations of the cross sections, we have constructed an adequate wavefunction by considering a bigger box of

30 au containing 128 molecules of water (to reproduce the mentioned experimental density). The resulting wavefunction does satisfy the asymptotic condition, i.e. it almost vanishes at and beyond the box walls. In this way, it is ensured that the initial bound wavefunction is mainly concentrated within the finite volume of the simulation box. This procedure gives an average ionization energy equal to 8.2 eV for the calculated $1B_1$ orbital. It must be mentioned that this type of calculation with bigger systems requires a considerable computational effort and CPU time.

2.2. Multiple differential cross sections

We develop a simple monoelectronic approximation that permits the reduction of the multielectronic problem into a one *active* electron problem. Several previous studies have employed this approximation with success to tackle multielectronic systems ([28], see also [29] for a review) and even liquid water [17]. This is justified by the fact that at the high and intermediate impact energies considered, there is no appreciable relaxation of the target during the effective collision time.

Under these assumptions, eight-fold multiple differential cross sections (8DCS) for single ionization of the *active* electron for a coplanar geometry at a fixed molecule orientation are obtained as

$$\sigma^{(8)}(\alpha,\beta,\gamma) = \frac{\mathrm{d}\sigma}{\mathrm{d}\Omega_{mol}\,\mathrm{d}\Omega_e\,\mathrm{d}\Omega_s\,\mathrm{d}E_e} = N(2\pi)^4\frac{k_e k_s}{k_i}\,|\langle\Psi_f^-|\,V_i\,|\psi_i\rangle|^2, \qquad (4)$$

where ψ_i and Ψ_f^- are the initial and the final wavefunctions (the latter with correct boundary conditions), respectively, and V_i is the perturbation in the initial channel. k_i, k_s and k_e are the incident, scattered and ejected electron momenta, respectively. Moreover, $\mathrm{d}\Omega_s$ and $\mathrm{d}\Omega_e$ denote the solid angles corresponding to k_s and k_e, respectively, whereas $\mathrm{d}\Omega_{\mathrm{mol}} = \sin\beta\ \mathrm{d}\alpha\ \mathrm{d}\beta\ \mathrm{d}\gamma$ with α,β,γ being the Euler angles of the water molecule described in the laboratory reference frame. As we are interested in asymmetric kinematic conditions, exchange effects are not taken into account in our model. Thus, $N = 2$ gives the number of electrons in the considered molecular orbital.

The initial wavefunction is chosen as

$$\psi_i = \frac{\mathrm{e}^{\mathrm{i}\mathbf{k}_i.\mathbf{R}}}{(2\pi)^{3/2}}\Phi_i(\mathbf{r};\alpha,\beta,\gamma), \qquad (5)$$

where $\mathbf{R}$ and $\mathbf{r}$ are the position vectors of the incident and *active* electrons, respectively, with respect to the centre of mass of the molecule. The initial molecular orbital of liquid water Φ_i is obtained through the use of Wannier orbitals [18] and the incident electron is described by a plane wave.

The final-state wavefunction is chosen as

$$\Psi_f^- \cong \frac{\mathrm{e}^{\mathrm{i}\mathbf{k}_s.\mathbf{R}}}{(2\pi)^{3/2}}C(k_e,\mathbf{r},\nu), \qquad (6)$$

where the continuum Coulomb wavefunction

$$C(\mathbf{k},\mathbf{r},\nu) = \Gamma(1-\mathrm{i}\nu)\,\frac{\mathrm{e}^{\mathrm{i}\mathbf{k}.\mathbf{r}}}{(2\pi)^{3/2}} \times \mathrm{e}^{-\pi\nu/2}\ {}_1F_1[\mathrm{i}\nu;1;-\mathrm{i}(kr+\mathbf{k}.\mathbf{r})] \qquad (7)$$

describes the ionized electron in the final channel in the field of the residual target at asymptotically large distances, with ${}_1F_1$ being the confluent hypergeometric function and $\nu = -Z^*/k = -1/k$ the corresponding Sommerfeld parameter. The charge $Z^* = 1$ takes into account the fact that the *passive* electrons produce a complete screening of the nuclear charges of the molecule at asymptotically large distances giving as a result a residual target with a net charge equal to unity.

The perturbation in the initial channel is taken as

$$V_i = \frac{1}{|\mathbf{r}-\mathbf{R}|} - \frac{1}{R} = \frac{1}{r_p} - \frac{1}{R} \qquad (8)$$

with $r_p = |\mathbf{r}-\mathbf{R}|$. This perturbation is in accordance with the choice of the initial wavefunction and with the following approximation. We neglect the spatial distribution of the nuclei and *passive* electrons in the water molecule, obtaining an average for the interaction of the projectile with these particles. Thus, we consider the interaction of the projectile with a net charge equal to unity that is equivalent to consider a total screening of the charge of the nuclei by the *passive* electrons. In this approximation, the short range part of the real interaction is neglected. This approximation was used by several authors, see for instance [19] for the gas phase and [17] for the liquid phase.

Integrating the 8DCS given by equation (4) over the Euler angles, we obtain five-fold differential cross sections (5DCS) averaged over all possible molecular orientations:

$$\sigma^{(5)} = \frac{\mathrm{d}\sigma}{\mathrm{d}\Omega_e\mathrm{d}\Omega_s\mathrm{d}E_e} = \frac{1}{8\pi^2}\int\sigma^{(8)}(\alpha,\beta,\gamma)\sin\beta\ \mathrm{d}\alpha\ \mathrm{d}\beta\ \mathrm{d}\gamma. \qquad (9)$$

To compute the 8DCS and 5DCS, numerical quadratures are performed within the simulation box.

3. Results

We apply our model of single ionization of liquid water to the case of electrons ejected from the $1B_1$ orbital. In particular, we consider coplanar geometries in which the incident, scattered and ejected momenta lie all in the same plane. Moreover, we analyse only cases of asymmetric kinematic conditions for the scattered and ejected electrons (ejection energies of some eV). In what follows, we obtain 8DCS for definite orientations of the molecule. As no theoretical predictions exist for oriented molecules in the liquid phase, we compare with the available results for the gas one. Our aim is to validate our wavefunctions and to ensure that our model describes the most important physical characteristics of the reaction. Moreover, we contrast our predictions for averaged oriented molecules with measurements for the gas phase as experimental results for the liquid state are not published.

3.1. MDCS for fixed molecular orientation: 8DCS

In this section, we present 8DCS for fixed-in-space water molecules as a function of the ejection angle θ_e. We consider a collision system of incident energy $E_i = 250$ eV and ejected

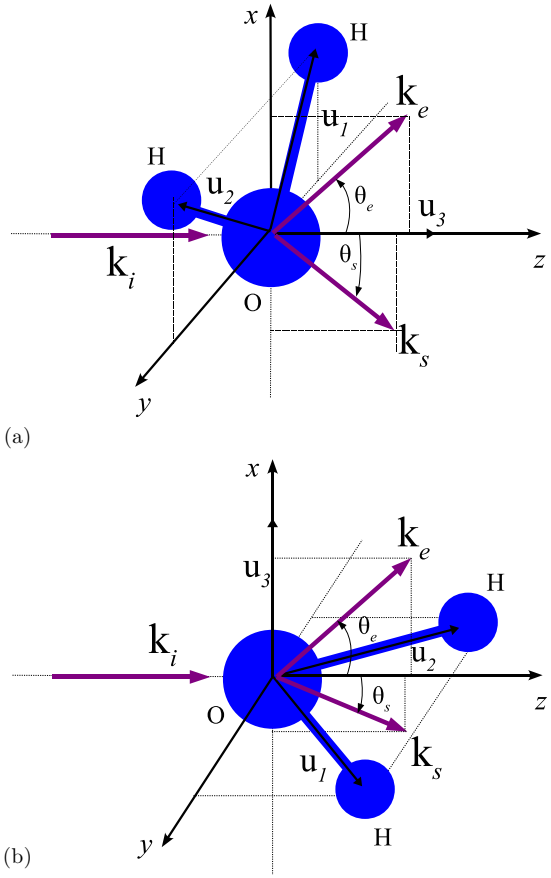

Figure 1. Fixed-in-space molecule configurations considered in this work. The molecules are oriented perpendicularly to the collision plane defined by the k_i and k_s directions. Unit vectors $\mathbf{u}_1$ and $\mathbf{u}_2$ define the molecular plane. (a) *Normal I* orientation. (b) *Normal II* orientation.

energy $E_e = 5$ eV. Moreover, we study two particular cases in which the target molecule is oriented with its molecular plane perpendicular to the collision one defined by both the incident and scattering directions. These configurations are denoted as *normal I* and *normal II*, and shown in figures 1(a) and (b), respectively. The molecular plane is defined by the unit vectors $\mathbf{u}_1$ and $\mathbf{u}_2$ (see figure 1). The incident direction is chosen along the z-axis. For the *normal I* orientation, the molecular plane is contained in the xy plane, while for the *normal II* configuration, it lies in the yz plane. These molecular orientations correspond to the Euler rotations $R_0(\theta, 0^\circ, 0^\circ)$ and $R_0(\theta, 90^\circ, 180^\circ)$, respectively, with θ being the demiangle between $\mathbf{u_1}$ and $\mathbf{u_2}$. The rotation operator is defined as $R_0(\alpha, \beta, \gamma) = R_{z''}(\gamma)R_{y'}(\beta)R_z(\alpha)$ [30].

Firstly, we compare our calculations for oriented molecules with the ones for the gas phase obtained from [19] as no predictions exist for the liquid phase. It is worthy to mention that in those predictions unfortunately only the term $1/r_p$ of the perturbation given by equation (8) was taken into account. Therefore, in order to make the comparison possible, we present in figures 2 and 3 our 8DCS obtained with only the $1/r_p$ term of the perturbation that is responsible for the interaction between the incident and the active electrons. As is well known, this interaction is crucial to describe the classical mechanism that gives place to the binary peak. However, the

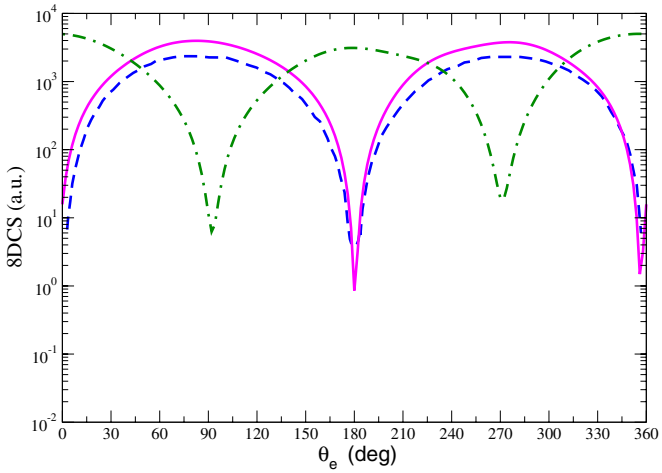

Figure 2. 8DCS per electron for the $1B_1$ orbital as a function of the ejection angle for the fixed molecular orientations depicted in figure 1. The incident and the ejection energies are $E_i = 250$ eV and $E_e = 5$ eV, respectively, whereas $\theta_s = 0^\circ$. Only the term $1/r_p$ is considered in the calculations (see the text). Full line presents results for the *normal II* orientation. Dash-dotted line presents results for the *normal I*. Dashed line: results for the gas phase from [19].

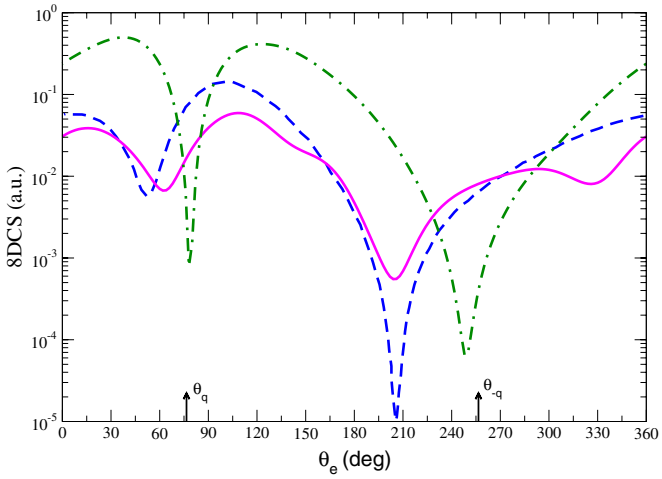

Figure 3. Same as figure 2 but $\theta_s = 15^\circ$. The arrows indicate the angular positions of $\mathbf{q}$ and $-\mathbf{q}$.

full perturbation given by equation (8) is necessary to describe correctly the physics involved in the reaction. We will see below that for instance the neglected term $1/R$ is of most importance to represent the recoil peak in the liquid phase in the same way as in the gas phase. The only reason for neglecting it in our 8DCS, shown in figures 2 and 3, is to allow a comparison with the previous results from [19].

Therefore in figures 2 and 3, we show our calculations for fixed scattering angles $\theta_s = 0^\circ$ and $\theta_s = 15^\circ$, respectively, for the two orientations considered in figure 1. We also include in the figures the mentioned previous results for the gas phase from [19]. We make the comparison only for the *normal II* orientation since there are no predictions for our *normal I* orientation.

We observe good qualitative agreement between our results and the corresponding ones for the gas phase [19]. For $\theta_s = 0^\circ$, the momentum transfer is small ($q = 0.11$ au)

and the reaction is mostly dipolar in nature. Then, for *normal II* orientation, the relative maxima located at $\theta_e = 90^\circ$ and 270° as well as the relative minima at $\theta_e = 0^\circ$ and 180° may be explained in terms of the high directional character of the $1B_1$ orbital. For this orientation, the $1B_1$ orbital is directed along the x-axis, where electron ejection is greater, whereas its nodal plane lies in the yz-plane, decreasing the ejection in the z-direction. In contrast, for the case of $\theta_s = 15^\circ$ considered in figure 3, the momentum transfer is much larger ($q = 1.1$ au) and the ionization process exhibits the typical features of a binary collision regime. Indeed, the relative maxima are located at about the classical directions of ejection given by the binary and recoil peaks. In the binary region, we observe a relative minimum around the classical position for the binary peak ($\theta_e = 76.5^\circ$ and 75.7° for the liquid and gas phases, respectively) giving place to a two-lobe structure. Another minimum is observed at about $\theta_e = 210^\circ$ that also appears for the gas phase [19] but in a less pronounced fashion. This behaviour may also be attributed to the strong p character of the $1B_1$ orbital: its marked directionality does not favour electron ejection in the momentum transfer nor in the backward directions in both thermodynamical phases. For the *normal I* orientation (dash-dotted lines), the behaviour of the 8DCS is similar to the one described above. In this case, the nodal plane of the orbital lies in the xy-plane disfavouring the electron ejection in the x-direction. For $\theta_s = 0^\circ$, the maxima and minima positions are shifted 90° with respect to the ones for the *normal II* orientation. We find relative maxima at $\theta_e = 0^\circ$ (or 360°) and 180°, and a relative minimum at 90°. For $\theta_s = 15^\circ$, relative maxima appear displaced to the binary region, with a pronounced minimum about the classical position of the binary peak, giving place to a two-lobe structure in this region. In the recoil region, we found a deeper minimum about the recoil peak position.

Although not shown here, we have also analysed another orientation in which the molecular plane is contained in the collision one. The respective cross sections are almost two orders of magnitude lower than the corresponding to the *normal* orientations. This may be understood taking into account that for this *coplanar* orientation, the nodal plane of the $1B_1$ orbital coincides with the collision one, reducing the probability of ionization in comparison with the *normal* orientations studied here.

Finally, in order to get a complete description of the problem, we show in figures 4 and 5 the results obtained with the full perturbation given by equation (8) for $\theta_s = 0^\circ$ and $\theta_s = 15^\circ$, respectively. In both figures we consider the case corresponding to the *normal I* configuration. We include the contributions to the cross sections given by the $1/R$ and $1/r_p$ terms of the perturbation. Similar considerations to the ones given for the $1/r_p$ term may be applied to explain the shape of the results obtained by considering only the $1/R$ term in the perturbation. The behaviour of the cross sections computed with the full perturbation is then given by the interplay between both $1/R$ and $1/r_p$ terms.

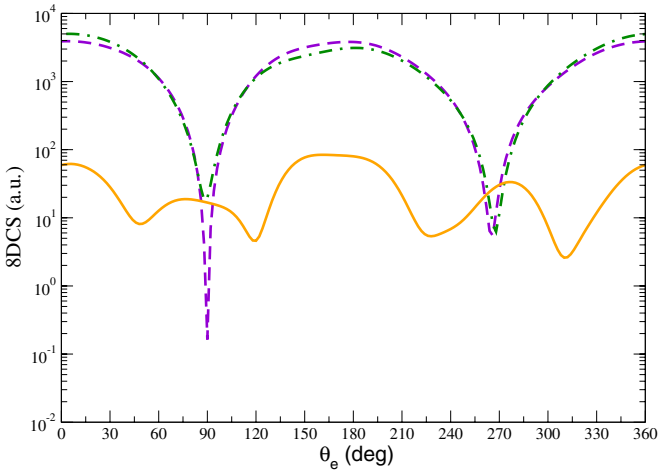

Figure 4. 8DCS per electron for the $1B_1$ orbital as a function of the ejection angle for the *normal I* orientation. The incident and the ejection energies are $E_i = 250$ eV and $E_e = 5$ eV, respectively, whereas $\theta_s = 0^\circ$. Full line: full perturbation contribution. Dashed line: $1/R$ contribution. Dash-dotted line: $1/r_p$ contribution.

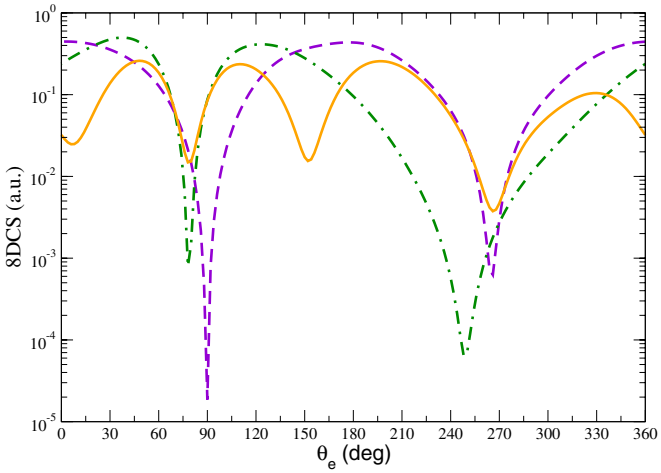

Figure 5. Same as figure 4 but $\theta_s = 15^\circ$.

3.2. MDCS averaged over all molecular orientations: 5DCS

In this section, we present 5DCS corresponding to the $1B_1$ orbital as a function of the ejection angle θ_e, and for several incident and ejected electron energies. At variance with the preceding section, we always include the full perturbation given by equation (8) in obtaining the cross sections. We compare them with previous theoretical and experimental results for randomly oriented water vapour molecules.

In figures 6 and 7, we show our 5DCS for liquid water at incident energies $E_i = 67.6$ eV and $E_i = 107.6$ eV, respectively. In both cases, the ejection energy is $E_e = 5$ eV, whereas the scattering angle is fixed at $\theta_s = 22^\circ$. We also include in the figures experimental results for the gas phase [13]. At both incident energies, we observe good qualitative agreement between our 5DCS and experiments. In spite of the fact that a molecule in the liquid phase does not have the same symmetry properties as a vapour molecule, our 5DCS present a rather small degree of asymmetry with respect to the momentum transfer direction. At $E_i = 67.6$ eV, our

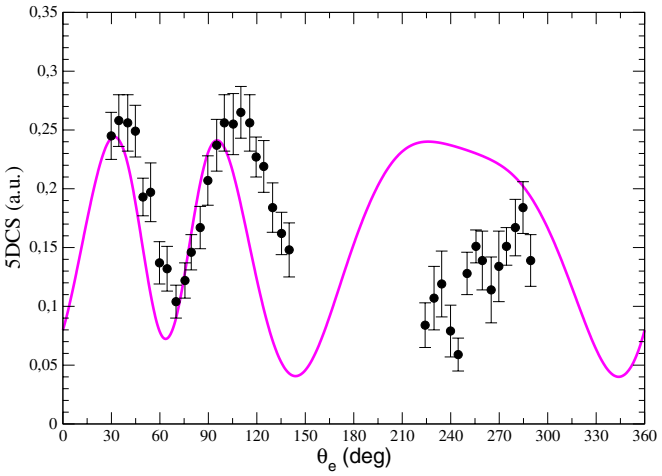

Figure 6. 5DCS of ionization of liquid water molecules from the $1B_1$ orbital as a function of the ejection angle. The incident and ejection energies are $E_i = 67.6$ eV and $E_e = 5$ eV, respectively, whereas the scattering angle is fixed at $\theta_s = 22^\circ$. Full line presents results. Dots: normalized gas phase measurements from [13].

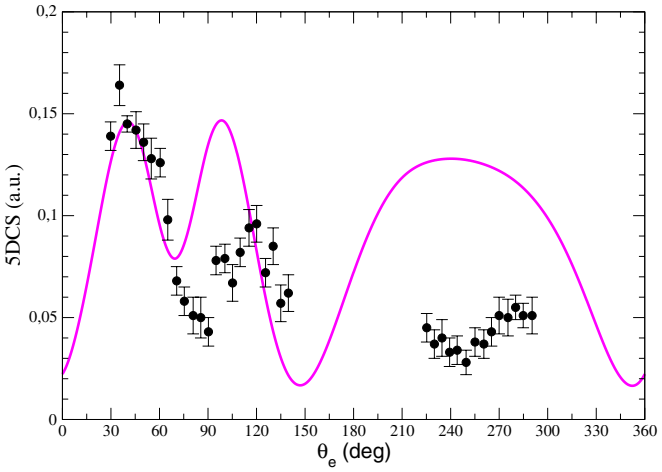

Figure 7. Same as figure 6 but incident energy $E_i = 107.6$ eV.

5DCS present an almost symmetric two-lobe structure that resembles the one of the vapour experiments. At variance, at $E_i = 107.6$ eV, the two-lobe structure of our 5DCS is still quite symmetric whereas a marked dissymmetry is observed in the measurements. Concerning the recoil region, we can see in both figures the presence of structures in the experimental results. Our calculations also show a broad peak at these angular values. However, if the $1/R$ term was neglected in the perturbation given by equation (8), no structure at all would appear as in the calculated cross sections for gas presented in [21] where this term was disregarded. So, it is clear that its inclusion is mandatory to describe the recoil angular region. As a matter of fact, when the mentioned cross sections for gas of [21] are corrected by incorporating the $1/R$ term in the perturbation, they exhibit a recoil peak in agreement with experiments [31]. Now, it can be seen that for the two incident energies considered, our 5DCS do not follow the trend of experiments in the recoil region. As no liquid experiments are available, we cannot establish if these discrepancies indicate a different behaviour between the liquid and gas phases, or

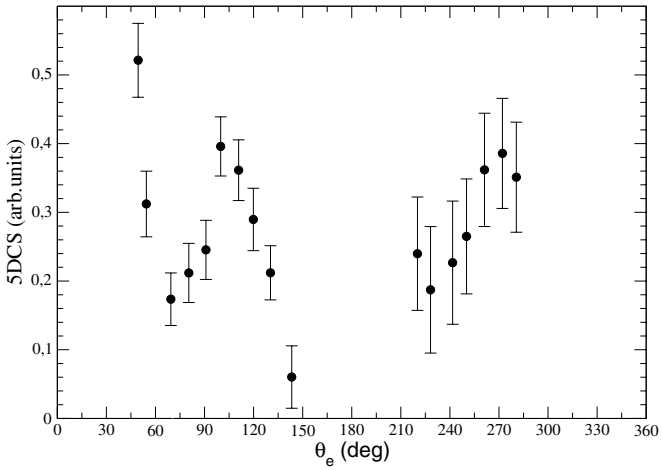

Figure 8. Summed experimental 5DCS for $1b_1$ and $3a_1$ orbitals of random water molecules in the gas phase for an incident energy $E_i = 250$ eV, ejected energy $E_e = 10$ eV and scattering angle $\theta_s = 15^\circ$ extracted from [21] (as measurements are not absolute, we have normalized them conveniently).

if they come from the approximate description of our model around the recoil peak. However, it must be noted that other theoretical predictions give also a recoil peak analogous to the one of our results at kinematic conditions not very far from the ones analysed in figures 4 and 5 as we will see below. In relation to the recoil region, we show in figure 8 experimental results for the gas phase [21] corresponding to the summed contributions of the most external $1b_1$ and $2a_1$ orbitals as the experiments were not able to resolve their difference in energy in the whole angular domain. These measurements were obtained on a relative scale so we have normalized them conveniently. Interestingly, similar structures to the ones observed in figures 6 and 7 also appear now in the recoil region. So, we compare in the following our cross sections with experimental results around the binary peak where resolution is enough to discriminate the $1b_1$ and $2a_1$ contributions.

In figure 9, we report our 5DCS for an incident energy $E_i = 250$ eV, ejected energy $E_e = 10$ eV and scattering angle $\theta_s = 15^\circ$. We also displayed in the figure experimental results (on a relative scale) at the binary region (where the resolution in energy is enough to separate them from the $2a_1$ ones) for the $1b_1$ orbital of the gas phase [21] as well as theoretical results for both liquid and gas phases. Our results agree qualitatively well with experiments and exhibit the characteristic two-lobe structure associated with the p orbital. Also, our 5DCS are in good qualitative agreement with the results for the gas phase given by the 1CW model [31]. In this calculation, the initial state is represented as in [19] by using a plane wave for the incident electron and Moccia's molecular wavefunction for the bound state of the target in the gas phase. The final state is described as the product of a plane wave for the scattered electron and a Coulomb wavefunction with effective ionic charge $Z^* = 1$ for the ionized electron. We recall that in the 1CW model, the $1/R$ term of the perturbation is included in the computations of 5DCS.

We also include in figure 9 recent results (FBA-CW model) developed in the framework of the first Born

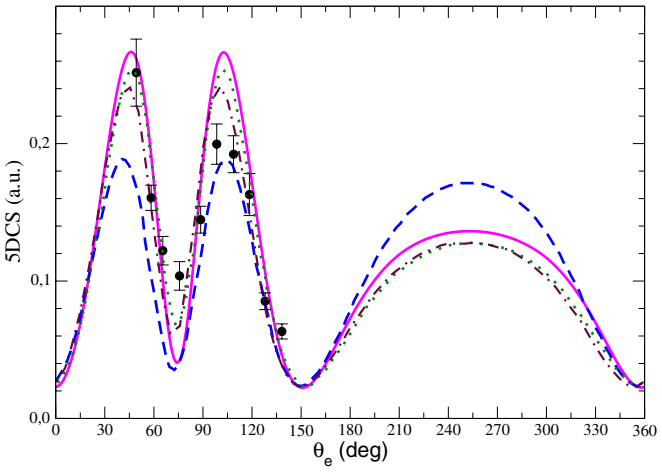

Figure 9. 5DCS for the ionization from the $1B_1$ liquid water orbital. The incident energy is $E_i = 250$ eV, the ejected energy is $E_e = 10$ eV and the scattering angle is $\theta_s = 15°$. Full line presents results. Dots: gas phase experiments [21]. Dashed line: 1CW results for the gas phase [31]. Dot-dashed line: FBA-CW results for the liquid phase [17]. Dotted line: FBA-CW results for the gas phase [17].

approximation for both the liquid and gas phases [17]. This model is quite similar to ours differing in the description of the molecular states. In the FBA-CW calculations, the initial orbitals for the liquid phase are described in a simpler manner by using a monocentric development of Gaussian expansions. There is general qualitative agreement among all theoretical predictions. Moreover, inspection of figure 9 leads to the conclusion that all calculations give place to binary and recoil peaks located around the classical angular positions. Despite the important differences in their physical properties, the FBA-CW predictions for both phases are practically the same. Contrarily, appreciable discrepancies may be seen between our results and the ones corresponding to the gas phase given by the 1CW and FBA-CW approximations. In particular, the height of the 1CW two-lobe structure for the gas phase in the binary region is approximately 50% less than the one given for our 5DCS for the liquid.

Finally, good agreement is observed between our predictions and the FBA-CW ones for the liquid phase although small differences are observed in the binary and recoil peaks. In general, the results for the liquid phase are greater than the ones for the vapour. This is attributed in [17] to the following fact. Due to the polarization effect provoked by the surrounding molecules, the orbital $1B_1$ of the liquid is more diffuse than the $1b_1$ of the gas phase giving place to greater 5DCS in the binary region.

4. Conclusions

We have studied ionization of water molecules in the liquid phase by fast electron impact by means of a simple first-order model through an independent electron approximation. For the first time in these kind of studies, the wavefunction of a single molecule in the liquid phase is represented through the use of Wannier orbital techniques [18]. The results obtained so far show that the main physical features observed in experiments for vapour (such as binary and recoil peaks) are similar to the ones predicted by our model. There is also good qualitative agreement with previous theoretical results for liquid water obtained through the use of first-order approximations. These facts validate the use of the wavefunctions here employed for the liquid phase and are encouraging to extend our work to the other orbitals of liquid water. This task is in progress and once finished may be useful to understand the dynamics of the (e, 2e) reaction involved. It is worthy to note that no relevant differences are found between the 5DCS obtained in previous works [17] for the gas and liquid phases despite their substantially different physical properties. This puts in evidence the need of more theoretical work describing in a proper manner the wavefunctions involved in the calculations of 5DCS. In this way, trusted 5DCS will be available to feed simulation codes for the deposition of energy in the living matter in order to understand the effect of ionizing radiations on the biological structures.

Acknowledgments

The authors acknowledge financial support from the SETCIP-ECOS-SUD Program A02E04, the Agencia Nacional de Promoción Científica y Tecnológica (PICT No. 01912) and the Consejo Nacional de Investigaciones Científicas y Técnicas de la República Argentina (PIP No. 11220090101026). The authors also thank the Centre Informatique National de l'Enseignement Supérieur (GENCI-CINES n° gps2369 Montpelier, France) and the Centro Científico Tecnológico Rosario (Argentina) for the computing resources and services.

References

[1] Goodhead D T and Nikjoo H 1989 *Int. J. Radiat. Biol.* **55** 513
[2] Nikjoo H, Uehara S, Wilson W E, Hoshi M and Goodhead D T 1998 *Int. J. Radiat. Biol.* **73** 355
[3] Boudaiffa B, Cloutier P, Hunting D, Huels M A and Sanche L 2000 *Science* **287** 1658
[4] Schutten J, de Heer F J, Moustapha H R, Boerboom A J H and Kistenmaker J 1966 *J. Chem. Phys.* **44** 3924
[5] Opal C B, Peterson W K and Beaty E C 1971 *J. Chem. Phys.* **55** 4100
[6] Opal C B, Beaty E C and Peterson W K 1972 *Data* **4** 209
[7] Vroom D A and Palmer R L 1977 *J. Chem. Phys.* **66** 3720
[8] Bolarisadeh M A and Rudd M E 1986 *Phys. Rev.* A **33** 882
[9] Hollman K W, Kerby G W III, Rudd M E, Miller J H and Manson S T 1988 *Phys. Rev.* A **38** 3299
[10] Straub H C, Lindsay B G, Smith K A and Stebbings R F 1998 *J. Chem. Phys.* **108** 109
[11] Itikawa Y and Mason N G 2005 *J. Phys. Chem. Ref. Data* **34** 1
[12] Frémont F, Hajaji A, Chesnel J-Y, Leprince P, Porée F, Gervais B and Hennecart D 2006 *Phys. Rev.* A **74** 012717
[13] Kaiser C, Spieker D, Gao J, Hussey M, Murray A and Madison D H 2007 *J. Phys. B: At. Mol. Opt. Phys.* **40** 2563–76
[14] Hafied H, Eschenbrenner A, Champion C, Ruiz-López R F, Dal Cappello C, Charpentier I and Hervieux P A 2007 *Chem. Phys. Lett.* **439** 55
[15] Nikjoo H, Goodhead D T, Charlton D E and Paretzke H G 1991 *Int. J. Radiat. Biol.* **60** 739
[16] Fojón O A, de Sanctis M L, Vuilleumier R, Stia C R and Politis M-F 2011 *J. Phys.: Conf. Ser.* **288** 012010

[17] Champion C 2010 *Phys. Med. Biol.* **55** 11
[18] Hunt P, Sprik M and Vuilleumier R 2003 *Chem. Phys. Lett.* **376** 68
[19] Champion C, Hanssen J and Hervieux P A 2001 *Phys. Rev.* A **63** 052720
Champion C, Hanssen J and Hervieux P A 2005 *Phys. Rev.* A **72** 059906
[20] Moccia R 1964 *J. Chem. Phys.* **40** 2186
[21] Milne-Brownlie D S, Cavanagh S J, Lohmann B, Champion C, Hervieux P A and Hanssen J 2004 *Phys. Rev.* A **69** 032701
[22] Marzari N and Vanderbilt D 1997 *Phys. Rev.* B **56** 12847
[23] Silvestrelli S, Marzari N, Vanderbilt D and Parrinello M 1998 *Solid State Commun.* **107** 7
[24] Vuilleumier R and Sprik M 2001 *J. Chem. Phys.* **115** 3454
[25] Silvestrelli S 1999 *Phys. Rev.* B **59** 9703
[26] Grossman J C, Schwegler E, Draeger E W and Galli G 2004 *J. Chem. Phys.* **120** 300
[27] Rotenberg B, Salanne M, Simon C and Vuilleumier R 2010 *Phys. Rev. Lett.* **104** 138101
[28] Champion C, Lekadir H, Galassi M E, Fojón O, Rivarola R D and Hanssen J 2010 *Phys. Med. Biol.* **55** 6053
[29] Stolterforht N, DuBois R D and Rivarola R D 1997 *Electron Emission in Heavy Ion–Atom Collisions* ed G Ecker, P Lambropoulos, I I Sobelman and H Walther (Berlin: Springer)
[30] Messiah A 1983 *Mecánica cuántica* vol 2 (Madrid: Tecnos)
[31] Champion C, Dal Cappello C, Houamer S and Mansouri A 2006 *Phys Rev.* A **73** 012717